PHYSICAL REVIEW D **89,** 095021 (2014)

Inferring the nature of the boson at 125–126 GeV

Arjun Menon[*]
Institute of Theoretical Science, University of Oregon, Eugene, Oregon 97403, USA

Tanmoy Modak,[†] Dibyakrupa Sahoo,[‡] and Rahul Sinha[§]
The Institute of Mathematical Sciences, Taramani, Chennai 600113, India

Hai-Yang Cheng[¶]
Institute of Physics, Academia Sinica, Taipei, Taiwan 11529, Republic of China
(Received 5 February 2013; revised manuscript received 28 March 2014; published 22 May 2014)

The presence of a bosonic resonance near 125 GeV has been firmly established at the Large Hadron Collider. Understanding the exact nature of this boson is a priority. The task now is to verify whether the boson is indeed the scalar Higgs as proposed in the Standard Model of particle physics, or something more esoteric as proposed in the plethora of extensions to the Standard Model. This requires a verification that the boson is a $J^{PC} = 0^{++}$ state with couplings precisely as predicted by the Standard Model. Since a non-Standard Model boson can in some cases mimic the Standard Model Higgs in its couplings to gauge bosons, it is essential to rule out any anomalous behavior in its gauge couplings. We present a step by step methodology to determine the properties of this resonance without making any assumptions about its couplings. We present the analysis in terms of uniangular distributions which lead to angular asymmetries that allow for the extraction of the couplings of the 125–126 GeV resonance to Z bosons. We show analytically and numerically, that these asymmetries can unambiguously confirm whether the new boson is indeed the Standard Model Higgs boson.

DOI: 10.1103/PhysRevD.89.095021 PACS numbers: 12.60.-i, 14.80.Bn, 14.80.Ec

I. INTRODUCTION

A new bosonic resonance with a mass of about 125 GeV has recently been observed at the Large Hadron Collider by both ATLAS Collaboration [1,2] and CMS Collaboration [3–5]. The mass of the resonance is suggestive that this resonance is the Higgs boson that should exist in the Standard Model (SM) of particle physics as a spin zero parity-even resonance. Significant effort is now directed at determining the properties and couplings of this new resonance to confirm that it is indeed the Higgs boson of the Standard Model. In this work we specify this new boson by the symbol H and we call it the Higgs, even though it has not been proved to be the Higgs of the Standard Model. This resonance is observed primarily in three decay channels $H \to \gamma\gamma$, $H \to ZZ$ and $H \to WW$, where one (or both) of the Z's and W's are off-shell. It is well known that the spin and parity of the resonance and its couplings can be determined by studying the momentum and angular distributions of the decay products. Indeed there is little doubt that a detailed numerical fit to the invariant masses of decay products and their angular distributions will reveal the true nature of this resonance. However, a detailed study of the angular distributions requires large statistics and may not be feasible currently. Several studies existed in the literature before the discovery of this new resonance [6–36] and yet several papers have appeared recently on strategies to determine the spin and parity of the resonance [37–50]. Yet, there is no clear conclusion on the step by step methodology to determine these properties and convincingly establish that the new resonance is indeed the Standard Model Higgs boson. The recent result [5] from CMS Collaboration on the determination of spin and parity of the new boson is not conclusive.

In this paper we are exclusively concerned with Higgs decaying to four charged leptons, which proceeds via a pair of Z bosons: $H \to ZZ \to (\ell_1^-\ell_1^+)(\ell_2^-\ell_2^+)$, where ℓ_1, ℓ_2 are leptons e or μ. Since the Higgs is not heavy enough to produce two real Z bosons, we can have one real and another off-shell Z, or both the Z's can be off-shell. While we deal with the former case in detail our analysis applies equally well to the latter case. We find that only in a very special case dealing with $J^P = 2^+$ boson it is more likely that both the Z bosons are off-shell. We emphasize that the final state $(e^+e^-)(\mu^+\mu^-)$ is not equivalent to $(e^+e^-)(e^+e^-)$ or $(\mu^+\mu^-)(\mu^+\mu^-)$ as sometimes mentioned in the literature, since the latter final states have to be antisymmetrized with respect to each of the two sets of identical fermions in the final state. The antisymmetrization of the amplitudes is not done in our analysis and hence our analysis applies only to $(e^+e^-)(\mu^+\mu^-)$. We examine the angular distributions and

[*]aamenon@uoregon.edu
[†]tanmoyy@imsc.res.in
[‡]sdibyakrupa@imsc.res.in
[§]sinha@imsc.res.in
[¶]phcheng@phys.sinica.edu.tw

present a strategy to determine the spin and parity of H, as well as its couplings to the Z bosons with the least possible measurements. Since the decay mode $H \to \gamma\gamma$ has been observed, H is necessarily a boson and the Landau-Yang theorem [51,52] excludes that it has spin $J = 1$. Further, assuming charge conjugation invariance, the observation of $H \to \gamma\gamma$ also implies [10] that H is a charge conjugation $C = +$ state. In making this assignment of charge conjugation it is assumed that H is an eigenstate of charge conjugation. With the charge conjugation of H thus established we will only deal with the parity of H henceforth. We consider only spin-0 and spin-2 possibilities for the H boson. Higher spin possibilities need not be considered for a comparative study as the number of independent helicity amplitudes does not increase any more [15,53]. The process under consideration requires that Bose symmetry be obeyed with respect to exchange of the pair of Z bosons. This constrains the number of independent helicity amplitudes to be less than or equal to six. Even if the spin-J of H is higher (i.e. $J \geq 3$), the number of independent helicity amplitudes still remains six. However, the helicity amplitudes corresponding to higher spin states involve higher powers of momentum of Z, independent of the momentum dependence of the form factors describing the process. We will show that even for $J^P = 2^+$ under a special case only two independent helicity amplitudes may survive just as in the case of $J^P = 0^+$. The two cases are in principle indistinguishable unless one makes an assumption on the momentum dependence of the form factors involved.

We start by considering the most general decay vertex for both scalar and tensor resonances H decaying to two Z bosons. We evaluate the partial decay rate of H in terms of the invariant mass squared of the dilepton produced from the nonresonant Z and the angular distributions of the four lepton final state. We demonstrate that by studying three uniangular distributions one can almost completely determine the spin and parity of H and also explore any anomalous couplings in the most general fashion. We find that $J^P = 0^-$ and 2^- can easily be excluded. The $J^P = 0^+$ and 2^+ possibilities can also be easily distinguished, but may require some lepton invariant mass measurements if the most general tensor vertex is considered. Only if H is found to be of spin-2, a complete three angle fit to the distribution is required to distinguish between $J^P = 2^+$ and 2^-.

The determination of couplings and spin, parity of the boson is important as there are other spin-0 and spin-2 particles predicted, such as the $J = 0$ radion [54–60] and $J = 2$ Kaluza-Klein graviton [45,61–63], which can easily mimic the initial signatures observed so far. Such cases have already been considered in the literature even in the context of this resonance. Our analysis is most general and such extensions are limiting cases in our analysis as the couplings are defined by the model.

In Sec. II we lay out the details of our analysis, with Secs. II A and II B devoted exclusively to spin-0 Higgs and spin-2 boson respectively. A step by step comparison with detailed procedure to distinguish the spin and parity states of the new boson is discussed in Sec. II C. In Sec. II D we present a numerical study to demonstrate the discriminating power of the uniangular distribution analysis compared to the current approach [64,65]. We find that uniangular distribution is more powerful in discriminating between the scalar (0^+) and pseudoscalar (0^-) hypothesis.

We conclude emphasizing the advantage of our approach in Sec. III.

II. DECAY OF THE NEW RESONANCE TO FOUR CHARGED LEPTONS VIA TWO Z BOSONS

Let us consider the decay of H to four charged leptons via a pair of Z bosons:

$$H \to Z_1 + Z_2 \to (\ell_1^- + \ell_1^+) + (\ell_2^- + \ell_2^+),$$

where ℓ_1, ℓ_2 are leptons e or μ. As mentioned in the Introduction we assume ℓ_1 and ℓ_2 are not identical. The kinematics for the decay is as shown in Fig. 1. The Higgs at rest is considered to decay with the on-shell Z_1 moving along the $+\hat{z}$ axis and off-shell Z_2 along the $-\hat{z}$ axis. The decays of Z_1 and Z_2 are considered in their rest frame. The angles and momenta involved are as described in Fig. 1. The four-momenta of H, Z_1 and Z_2 are defined as P, q_1 and q_2 respectively. We choose Z_1 to decay to lepton pair $\ell_1^\pm$ with momentum k_1 and k_2 respectively and Z_2 to decay to $\ell_2^\pm$ with momentum k_3 and k_4 respectively.

Nelson [6–8] and Dell'Aquilla [7] realized the significance of studying angular correlations in this process with Higgs boson decaying to a pair of Z bosons for inferring the nature of the Higgs boson. References [12,14,15] were the first to extend the analysis to include higher spin possibilities so that any higher spin particle can effectively be distinguished from SM Higgs. We study similar angular correlations in this paper. We begin the study by considering the most general HZZ vertices for a $J = 0$ and a $J = 2$ resonance H. We shall first discuss the two spin possibilities separately. Later we will lay out the approach to distinguish them assuming the most general HZZ vertex.

A. Spin-0 Higgs

The most general HZZ vertex factor $V_{HZZ}^{\alpha\beta}$ for spin-0 Higgs is given by

$$V_{HZZ}^{\alpha\beta} = \frac{igM_Z}{\cos\theta_W}(ag^{\alpha\beta} + bP^\alpha P^\beta + ic\epsilon^{\alpha\beta\mu\nu}q_{1\mu}q_{2\nu}), \quad (1)$$

where θ_W is the *weak mixing angle*, g is the electroweak coupling, and a, b, c are some arbitrary form factors dependent on the four-momentum squares specifying the vertex. The vertex $V_{HZZ}^{\alpha\beta}$ is derived from an effective Lagrangian (see for example Ref. [66]) where higher dimensional operators contribute to the momentum

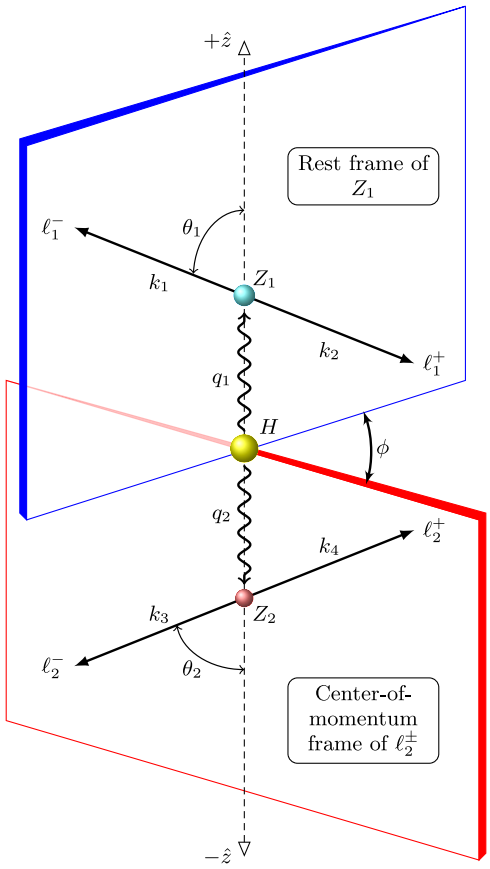

FIG. 1 (color online). Definition of the polar angles (θ_1 and θ_2) and the azimuthal angle (ϕ) in the decay of Higgs (H) to a pair of Z's, and then to four charged leptons: $H \to Z_1 + Z_2 \to (\ell_1^- + \ell_1^+) + (\ell_2^- + \ell_2^+)$, where $\ell_1, \ell_2 \in \{e, \mu\}$. It should be clear from the figure that $\vec{k}_1 = -\vec{k}_2$ and $\vec{k}_3 = -\vec{k}_4$. Since Z_2 is off-shell, we cannot go to its rest frame. However, given the momenta of ℓ_2^+ and ℓ_2^- we can always go to their center-of-momentum frame.

dependence of the form factors. Since the effective Lagrangian in the case of arbitrary new physics is not known, no momentum dependence of a, b and c can be assumed if the generality of the approach has to be retained. Approaches using constant values for the form factors therefore cannot provide unambiguous determination of spin-parity of the new boson. We emphasize that even though the momentum dependence of a, b and c is not explicitly specified, they must be regarded as being momentum dependent in general. In SM, however, a, b, c are constants and take the value $a = 1$ and $b = c = 0$ at tree level.

In Eq. (1) the term proportional to c is odd under parity and the terms proportional to both a and b are even under parity. Partial-wave analysis tells us that such a decay gets contributions from the first three partial waves, namely $\mathcal{S}$-wave, $\mathcal{P}$-wave and $\mathcal{D}$-wave. Since $\mathcal{S}$- and $\mathcal{D}$-waves are parity even while the $\mathcal{P}$-wave is parity odd, the term associated with c effectively describes the $\mathcal{P}$-wave contribution. The terms proportional to a and b are admixtures of $\mathcal{S}$- and $\mathcal{D}$-wave contributions. The decay of a spin-0 particle to two spin-1 massive particles is hence always described by three helicity amplitudes.

The decay under consideration is more conveniently described in terms of helicity amplitudes A_L, $A_\parallel$ and $A_\perp$ defined in the transversity basis as

$$A_L = q_1 \cdot q_2 a + M_H^2 X^2 b, \tag{2}$$

$$A_\parallel = \sqrt{2 q_1^2 q_2^2}\, a, \tag{3}$$

$$A_\perp = \sqrt{2 q_1^2 q_2^2}\, X M_H c, \tag{4}$$

where $\sqrt{q_1^2}$ and $\sqrt{q_2^2}$ are the invariant masses of the $\ell_1^\pm$ and $\ell_2^\pm$ lepton pairs respectively, i.e. $q_1^2 \equiv (k_1 + k_2)^2$, $q_2^2 \equiv (k_3 + k_4)^2$,

$$X = \frac{\sqrt{\lambda(M_H^2, q_1^2, q_2^2)}}{2 M_H}, \tag{5}$$

a, b and c are the coefficients that enter the most general vertex we have written in Eq. (1) and

$$\lambda(x, y, z) = x^2 + y^2 + z^2 - 2xy - 2xz - 2yz. \tag{6}$$

It should be remembered that the helicities $A_L, A_\parallel$ and $A_\perp$ are in general functions of q_1^2 and q_2^2, even though the functional dependence is not explicitly stated. The advantage of using the helicity amplitudes is that the helicity amplitudes are orthogonal. Our helicity amplitudes are defined in the transversity basis and thus differ from those given in Ref. [66]. Our amplitudes can be classified by their parity: A_L and $A_\parallel$ are parity even and $A_\perp$ is parity odd. This is unlike the amplitudes used in Ref. [66]. Throughout the paper we use linear combinations of the helicity amplitudes such that they have well defined parity. *This basis may be referred to as the transversity basis*. Even though we work in terms of helicity amplitudes in the transversity basis, we will show below, it is in fact possible to uniquely extract out the coefficients a, b, c which characterize the most general HZZ vertex for $J = 0$ Higgs.

We will assume that Z_1 is on-shell while Z_2 is off-shell, unless it is explicitly stated that both the Z bosons are off-shell. The off-shell nature of the Z is denoted by a superscript "*". One can easily integrate over q_1^2 using the narrow width approximation of the Z. The helicity amplitudes are then defined at $q_1^2 \equiv M_Z^2$ and q_2^2. In principle q_1^2 could also have been explicitly integrated out in both the cases when either Z_1 is off-shell or fully on-shell, resulting in some weighted averaged value of the helicities. The differential decay rate for the process $H \to Z_1 + Z_2^* \to (\ell_1^- + \ell_1^+) + (\ell_2^- + \ell_2^+)$, after integrating over q_1^2 (assuming Z_1 is on-shell or even otherwise) can now be written in terms of the angular distribution using the vertex given in Eq. (1) as

$$\frac{8\pi}{\Gamma_f}\frac{d^4\Gamma}{dq_2^2 d\cos\theta_1 d\cos\theta_2 d\phi} = 1 + \frac{|F_\parallel|^2 - |F_\perp|^2}{4}\cos 2\phi(1 - P_2(\cos\theta_1))(1 - P_2(\cos\theta_2))$$
$$+ \frac{1}{2}\mathrm{Im}(F_\parallel F_\perp^*)\sin 2\phi(1 - P_2(\cos\theta_1))(1 - P_2(\cos\theta_2))$$
$$+ \frac{1}{2}(1 - 3|F_L|^2)(P_2(\cos\theta_1) + P_2(\cos\theta_2)) + \frac{1}{4}(1 + 3|F_L|^2)P_2(\cos\theta_1)P_2(\cos\theta_2)$$
$$+ \frac{9}{8\sqrt{2}}(\mathrm{Re}(F_L F_\parallel^*)\cos\phi + \mathrm{Im}(F_L F_\perp^*)\sin\phi)\sin 2\theta_1 \sin 2\theta_2$$
$$+ \eta\left(\frac{3}{2}\mathrm{Re}(F_\parallel F_\perp^*)(\cos\theta_2(2 + P_2(\cos\theta_1)) - \cos\theta_1(2 + P_2(\cos\theta_2)))\right.$$
$$+ \frac{9}{2\sqrt{2}}\mathrm{Re}(F_L F_\perp^*)(\cos\theta_1 - \cos\theta_2)\cos\phi\sin\theta_1\sin\theta_2$$
$$\left. - \frac{9}{2\sqrt{2}}\mathrm{Im}(F_L F_\parallel^*)(\cos\theta_1 - \cos\theta_2)\sin\phi\sin\theta_1\sin\theta_2\right) - \frac{9}{4}\eta^2((1 - |F_L|^2)\cos\theta_1\cos\theta_2$$
$$+ \sqrt{2}(\mathrm{Re}(F_L F_\parallel^*)\cos\phi + \mathrm{Im}(F_L F_\perp^*)\sin\phi)\sin\theta_1\sin\theta_2), \quad (7)$$

where the *helicity fractions* F_L, $F_\parallel$ and $F_\perp$ are defined as

$$F_\lambda = \frac{A_\lambda}{\sqrt{|A_L|^2 + |A_\parallel|^2 + |A_\perp|^2}}, \quad (8)$$

where $\lambda \in \{L, \parallel, \perp\}$ and

$$\Gamma_f \equiv \frac{d\Gamma}{dq_2^2} = \mathcal{N}(|A_L|^2 + |A_\parallel|^2 + |A_\perp|^2), \quad (9)$$

with

$$\mathcal{N} = \frac{1}{2^4}\frac{1}{\pi^2}\frac{g^2}{\cos^2\theta_W}\frac{\mathrm{Br}_{\ell\ell}^2}{M_H^2}\frac{\Gamma_Z}{M_Z}\frac{X}{((q_2^2 - M_Z^2)^2 + M_Z^2\Gamma_Z^2)}, \quad (10)$$

where Γ_Z is the total decay width of the Z boson, $\mathrm{Br}_{\ell\ell}$ is the branching ratio for the decay of the Z boson to two massless leptons: $Z \to \ell^+\ell^-$ and we have used the narrow width approximation for the on-shell Z. We emphasize that with q_1^2 integrated out the helicity amplitudes A_λ and helicity fractions F_λ are functions only of q_2^2. In Eq. (7) η is defined as

$$\eta = \frac{2v_\ell a_\ell}{v_\ell^2 + a_\ell^2} \quad (11)$$

with $v_\ell = 2I_{3\ell} - 4e_\ell \sin^2\theta_W$ and $a_\ell = 2I_{3\ell}$, and $P_2(x)$ is the second degree Legendre polynomial:

$$P_2(x) = \frac{1}{2}(3x^2 - 1) \quad (\text{with } x \in \{\cos\theta_1, \cos\theta_2\}). \quad (12)$$

We have chosen to express the differential decay rate in terms of Legendre polynomials for $\cos\theta_1$ and $\cos\theta_2$ and Fourier series for ϕ. This ensures that each term in Eq. (7) is orthogonal to any other term in the distribution. The Legendre polynomials $P_m(\cos\theta_1)$ and $P_m(\cos\theta_2)$ satisfy the orthogonality condition since the range of $\cos\theta_1$ and $\cos\theta_2$ is -1 to 1, whereas that of ϕ is 0 to 2π. Our approach of using Legendre polynomials and the choice of helicity amplitudes in the transversity basis classified by parity form the cornerstone of our analysis. The same technique will be used in Sec. II B to analyze the spin-2 case.

An interesting observation in the scalar case is that the coefficients of $P_2(\cos\theta_1)$ and $P_2(\cos\theta_2)$ are identically equal to $\frac{1}{2}(1 - 3|F_L|^2)$ in both magnitude and sign. It is worth noting that the coefficients of $\cos 2\phi P_2(\cos\theta_1)$ and $\cos 2\phi P_2(\cos\theta_2)$ are also identically equal to $\frac{1}{4}(|F_\parallel|^2 - |F_\perp|^2)$ in both magnitude and sign.

Integrating Eq. (7) with respect to $\cos\theta_1$ or $\cos\theta_2$ or ϕ, the following uniangular distributions are obtained:

$$\frac{1}{\Gamma_f}\frac{d^2\Gamma}{dq_2^2 d\cos\theta_1} = \frac{1}{2} + T_2^{(0)}P_2(\cos\theta_1) - T_1^{(0)}\cos\theta_1, \quad (13)$$

$$\frac{1}{\Gamma_f}\frac{d^2\Gamma}{dq_2^2 d\cos\theta_2} = \frac{1}{2} + T_2^{(0)}P_2(\cos\theta_2) + T_1^{(0)}\cos\theta_2, \quad (14)$$

$$\frac{2\pi}{\Gamma_f}\frac{d^2\Gamma}{dq_2^2 d\phi} = 1 + U_2^{(0)}\cos 2\phi + V_2^{(0)}\sin 2\phi + U_1^{(0)}\cos\phi + V_1^{(0)}\sin\phi, \quad (15)$$

where

$$T_2^{(0)} = \frac{1}{4}(1 - 3|F_L|^2), \quad (16)$$

$$U_2^{(0)} = \frac{1}{4}(|F_\parallel|^2 - |F_\perp|^2), \quad (17)$$

$$V_2^{(0)} = \frac{1}{2}\mathrm{Im}(F_\parallel F_\perp^*), \tag{18}$$

$$T_1^{(0)} = \frac{3}{2}\eta\mathrm{Re}(F_\parallel F_\perp^*), \tag{19}$$

$$U_1^{(0)} = -\frac{9\pi^2}{32\sqrt{2}}\eta^2\mathrm{Re}(F_L F_\parallel^*), \tag{20}$$

$$V_1^{(0)} = -\frac{9\pi^2}{32\sqrt{2}}\eta^2\mathrm{Im}(F_L F_\perp^*), \tag{21}$$

are explicitly functions of q_2^2. The superscript (0) indicates the spin of H. Since $P_0(\cos\theta_{1,2})=1$, $P_1(\cos\theta_{1,2})=\cos\theta_{1,2}$, $P_2(\cos\theta_1)$, $\cos\phi$, $\sin\phi$, $\cos 2\phi$ and $\sin 2\phi$ are orthogonal functions, the coefficients of each of the terms can be extracted individually. We can also extract all the above coefficients in terms of asymmetries defined as below:

$$\begin{aligned} T_1^{(0)} &= \left(\int_{-1}^{0} - \int_{0}^{+1}\right) d\cos\theta_1 \left(\frac{1}{\Gamma_f}\frac{d^2\Gamma}{dq_2^2 d\cos\theta_1}\right) \\ &= \left(-\int_{-1}^{0} + \int_{0}^{+1}\right) d\cos\theta_2 \left(\frac{1}{\Gamma_f}\frac{d^2\Gamma}{dq_2^2 d\cos\theta_2}\right), \end{aligned} \tag{22}$$

$$T_2^{(0)} = \frac{4}{3}\left(\int_{-1}^{-\frac{1}{2}} - \int_{-\frac{1}{2}}^{+\frac{1}{2}} + \int_{+\frac{1}{2}}^{+1}\right) d\cos\theta_{1,2} \left(\frac{1}{\Gamma_f}\frac{d^2\Gamma}{dq_2^2 d\cos\theta_{1,2}}\right), \tag{23}$$

$$U_1^{(0)} = \frac{1}{4}\left(-\int_{-\pi}^{-\frac{\pi}{2}} + \int_{-\frac{\pi}{2}}^{+\frac{\pi}{2}} - \int_{+\frac{\pi}{2}}^{+\pi}\right) d\phi \left(\frac{2\pi}{\Gamma_f}\frac{d^2\Gamma}{dq_2^2 d\phi}\right), \tag{24}$$

$$U_2^{(0)} = \frac{1}{4}\left(\int_{-\pi}^{-\frac{3\pi}{4}} - \int_{-\frac{3\pi}{4}}^{-\frac{\pi}{4}} + \int_{-\frac{\pi}{4}}^{\frac{\pi}{4}} - \int_{\frac{\pi}{4}}^{\frac{3\pi}{4}} + \int_{\frac{3\pi}{4}}^{\pi}\right) d\phi \left(\frac{2\pi}{\Gamma_f}\frac{d^2\Gamma}{dq_2^2 d\phi}\right), \tag{25}$$

$$V_1^{(0)} = \frac{1}{4}\left(-\int_{-\pi}^{0} + \int_{0}^{+\pi}\right) d\phi \left(\frac{2\pi}{\Gamma_f}\frac{d^2\Gamma}{dq_2^2 d\phi}\right), \tag{26}$$

$$V_2^{(0)} = \frac{1}{4}\left(\int_{-\pi}^{-\frac{\pi}{2}} - \int_{-\frac{\pi}{2}}^{0} + \int_{0}^{+\frac{\pi}{2}} - \int_{+\frac{\pi}{2}}^{+\pi}\right) d\phi \left(\frac{2\pi}{\Gamma_f}\frac{d^2\Gamma}{dq_2^2 d\phi}\right). \tag{27}$$

As had already been realized from Eq. (7), the coefficients of $P_2(\cos\theta_1)$ and $P_2(\cos\theta_2)$ as well as the coefficients of $\cos\theta_1$ and $\cos\theta_2$ in Eqs. (13) and (14) are identical. This results in a maximum of 6 possible independent measurements $T_1^{(0)}$, $U_1^{(0)}$, $V_1^{(0)}$, $T_2^{(0)}$, $U_2^{(0)}$ and $V_2^{(0)}$ using uniangular analysis. For the decay under consideration, $v_\ell = -1 + 4\sin^2\theta_W$ and $a_\ell = -1$. Substituting the experimental value for the weak mixing angle: $\sin^2\theta_W = 0.231$, we get $\eta = 0.151$ and $\eta^2 = 0.0228$. Owing to such small values of η and η^2 it is unlikely that $T_1^{(0)}$, $U_1^{(0)}$ and $V_1^{(0)}$ can be measured using the small data sample currently available at LHC, reducing the number of independent measurable to three.

Using Eqs. (16) and (17) and the identity $|F_L|^2 + |F_\parallel|^2 + |F_\perp|^2 = 1$, the following solutions for $|F_L|^2$, $|F_\parallel|^2$ and $|F_\perp|^2$ are obtained:

$$|F_L|^2 = \frac{1}{3}(1 - 4T_2^{(0)}), \tag{28}$$

$$|F_\parallel|^2 = \frac{1}{3}(1 + 2T_2^{(0)}) + 2U_2^{(0)}, \tag{29}$$

$$|F_\perp|^2 = \frac{1}{3}(1 + 2T_2^{(0)}) - 2U_2^{(0)}. \tag{30}$$

We have shown that one can easily measure all the three helicity fractions using uniangular distributions. We can also measure $\mathrm{Im}(F_\parallel F_\perp^*)$, which is proportional to sine of the phase difference between the two helicity amplitudes $A_\parallel$ and $A_\perp$. In other words, we can also measure the relative phase between the parity-odd and parity-even amplitudes. Such a phase can arise if CP symmetry is violated in HZZ interactions or could indicate pseudo-time reversal violation arising from loop level contributions or rescattering effects akin to the strong phase in strong interactions. Since such a term requires contributions from both parity-even and parity-odd partial waves, $V_2^{(0)} = 0$ in SM. In the case of SM we have $a = 1$ and $b = c = 0$. Assuming narrow width approximation for the on-shell Z_1 we get

$$F_\perp = 0, \tag{31}$$

$$\frac{F_L}{F_\parallel} \equiv \mathsf{T} = \frac{M_H^2 - M_Z^2 - q_2^2}{2\sqrt{2}M_Z\sqrt{q_2^2}}. \tag{32}$$

Clearly, for the case of SM the term T has a characteristic dependence on $\sqrt{q_2^2}$. Demanding $F_\perp = 0$, we get

$$U_2^{(0)} = \frac{1}{6}(1 + 2T_2^{(0)}), \tag{33}$$

and

$$|\mathsf{T}| = \frac{1 - 4T_2^{(0)}}{2 + 4T_2^{(0)}}. \tag{34}$$

Thus for SM we can predict the experimental values for the coefficients $T_2^{(0)}$ and $U_2^{(0)}$ as

$$T_2^{(0)} = \frac{1}{4}\left(\frac{1 - 2|\mathsf{T}|}{1 + |\mathsf{T}|}\right), \qquad U_2^{(0)} = \frac{1}{4(1 + |\mathsf{T}|)}. \tag{35}$$

It is evident that $T_2^{(0)}$ and $U_2^{(0)}$ are functions of $\sqrt{q_2^2}$ alone and are uniquely predicted in the SM. $T_2^{(0)}$ and $U_2^{(0)}$ are pure

numbers for a given value of $\sqrt{q_2^2}$. Their variation with respect to $\sqrt{q_2^2}$ is shown in Fig. 2(a). It is clear from the plot that $T_2^{(0)}$ is always negative while $U_2^{(0)}$ is always positive in the SM. The variation of the helicity fractions with respect to $\sqrt{q_2^2}$ is shown in Fig. 2(b). Figure 2(c) also shows the variation of the normalized differential decay width of the SM Higgs decaying to four charged leptons via two Z bosons with respect to $\sqrt{q_2^2}$. Figure 2 contains all the vital experimental signatures of the SM Higgs and must be verified in order for the new boson to be consistent with the

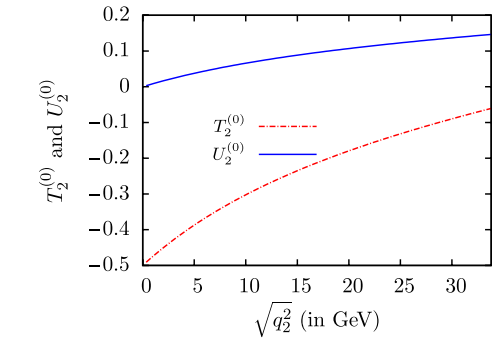

(a) Plot of $T_2^{(0)}$ and $U_2^{(0)}$ vs $\sqrt{q_2^2}$.

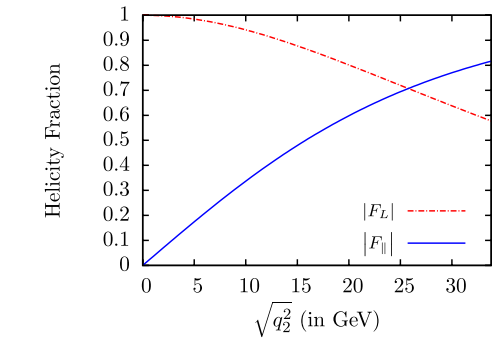

(b) Plot of F_L and $F_\parallel$ vs. $\sqrt{q_2^2}$.

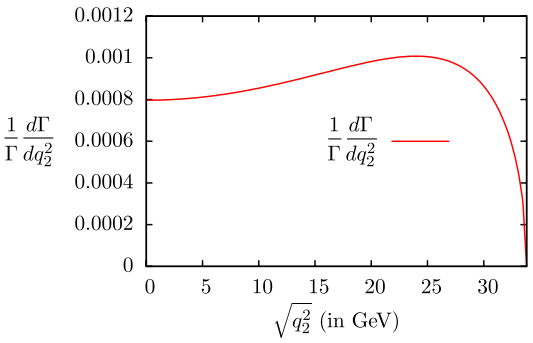

(c) Plot of $\frac{1}{\Gamma}\frac{d\Gamma}{dq_2^2}$ vs $\sqrt{q_2^2}$.

FIG. 2 (color online). Plots of various observables in SM only. We have used $M_H = 125$ GeV, $\sqrt{q_1^2} = 91.18$ GeV for the above plots. The integrated values for the observables $T_2^{(0)}$ and $U_2^{(0)}$ are uniquely predicted in SM at tree level to be -0.148 and 0.117 respectively.

SM Higgs boson. We emphasize that a nonzero measurement of $F_\perp$ will be a litmus test indicating a non-SM behavior for the Higgs. Furthermore, a nonzero $V_2^{(0)}$ would imply that the observed resonance is not of definite parity.

If we find the new boson to be of $J^{PC} = 0^{++}$, but still not exactly like the SM Higgs, then we need to know the values of a and b in the vertex factor of Eq. (1). It is easy to find that for a general 0^{++} boson, the values of both a and b are given by

$$a = \frac{F_\parallel \sqrt{\Gamma_f/\mathcal{N}}}{\sqrt{2} M_Z \sqrt{q_2^2}}, \tag{36}$$

$$b = \frac{\sqrt{\Gamma_f/\mathcal{N}}}{M_H^2 X^2}\left(F_L - \frac{M_H^2 - M_Z^2 - q_2^2}{2\sqrt{2} M_Z \sqrt{q_2^2}} F_\parallel\right). \tag{37}$$

For SM $a = 1$ and $b = 0$ at tree level only. At loop level even within SM these values would differ. It may be hoped that a and b determined in this way may enable testing SM even at one loop level once sufficient data is acquired. This is significant as triple-Higgs vertex contributes at one loop level and *measurement of b may provide the first verification of the Higgs-self coupling*. Even if the scalar boson is not a parity eigenstate but an admixture of even and odd parity states, Eqs. (36) and (37) can be used to determine a and b. We can determine c by measuring $F_\perp$:

$$c = \frac{F_\perp \sqrt{\Gamma_f/\mathcal{N}}}{\sqrt{2} M_Z \sqrt{q_2^2} M_H X}. \tag{38}$$

Therefore, it is possible to get exact solutions for a, b, c in terms of the experimentally observable quantities like F_L, $F_\parallel$, $F_\perp$ and Γ_f.

We want to stress that it is impossible to extract out both a and b by measuring only one uniangular distribution (corresponding to either $\cos\theta_1$ or $\cos\theta_2$), since the helicity amplitude A_L contains both a and b. Hence, it is not possible to conclude that the 0^{++} boson is a Standard Model Higgs by studying $\cos\theta_1$ or $\cos\theta_2$ distributions alone.

The current data set is limited and may allow binning only in one variable. We therefore examine what conclusions can be made if q_2^2 is also integrated out and only the three uniangular distributions are studied individually. As can be seen from Eqs. (36), (37) and (38) we can obtain some weighted averages of a and c. These equations will only allow us to verify whether $a = 1$ and $c = 0$. In addition the presence of any phase between the parity-even and parity-odd amplitudes can still be inferred from Eq. (18). The integrated values for the observables $T_2^{(0)}$ and $U_2^{(0)}$ are uniquely predicted in SM at tree level to be -0.148 and 0.117 respectively.

B. Spin-2 boson

As stated in the Introduction we shall use the same symbol H to denote the boson even if it is of spin-2. The most general HZZ vertex factor $V_{HZZ}^{\mu\nu;\alpha\beta}$ for spin-2 boson, with polarization $\epsilon_{(T)}^{\mu\nu}$ has the following tensor structure:

$$\begin{aligned} V_{HZZ}^{\mu\nu;\alpha\beta} &= A(g^{\alpha\nu}g^{\beta\mu}+g^{\alpha\mu}g^{\beta\nu})+B(Q^{\mu}(Q^{\alpha}g^{\beta\nu}+Q^{\beta}g^{\alpha\nu})+Q^{\nu}(Q^{\alpha}g^{\beta\mu}+Q^{\beta}g^{\alpha\mu}))+C(Q^{\mu}Q^{\nu}g^{\alpha\beta}) \\ &\quad -D(Q^{\alpha}Q^{\beta}Q^{\mu}Q^{\nu})+2iE(g^{\beta\nu}\epsilon^{\alpha\mu\rho\sigma}-g^{\alpha\nu}\epsilon^{\beta\mu\rho\sigma}+g^{\beta\mu}\epsilon^{\alpha\nu\rho\sigma}-g^{\alpha\mu}\epsilon^{\beta\nu\rho\sigma})q_{1\rho}q_{2\sigma} \\ &\quad +iF(Q^{\beta}(Q^{\nu}\epsilon^{\alpha\mu\rho\sigma}+Q^{\mu}\epsilon^{\alpha\nu\rho\sigma})-Q^{\alpha}(Q^{\nu}\epsilon^{\beta\mu\rho\sigma}+Q^{\mu}\epsilon^{\beta\nu\rho\sigma}))q_{1\rho}q_{2\sigma}, \end{aligned} \tag{39}$$

where ϵ_α and ϵ_β are the polarizations of the two Z bosons; A, B, C, D, E and F are arbitrary coefficients and Q is the difference of the four-momenta of the two Z's, i.e. $Q = q_1 - q_2$. Only the term that is associated with the coefficient A is dimensionless. The form of the vertex factor ensures that $P_\mu\epsilon_{(T)}^{\mu\nu} = P_\nu\epsilon_{(T)}^{\mu\nu} = 0$ and $g_{\mu\nu}\epsilon_{(T)}^{\mu\nu} = 0$, which stem from the fact that the field of a spin-2 particle is described by a symmetric, traceless tensor with null four-divergence. Here like the spin-0 case P is the sum of the four-momenta of the two Z's, i.e. $P = q_1 + q_2$. Since we are considering the decay of Higgs to two Z bosons, the vertex factor must be symmetric under the exchange of the two identical bosons. This is taken care of by making the vertex factor symmetric under simultaneous exchange of α, β and corresponding momenta of Z_1 and Z_2. The Lagrangian that gives rise to the vertex factor $V_{HZZ}^{\mu\nu;\alpha\beta}$ contains higher dimensional operators, which are responsible for the momentum dependence of the form factors.

In $V_{HZZ}^{\mu\nu;\alpha\beta}$ the terms that are proportional to E and F are parity odd and the rest of the terms in $V_{HZZ}^{\mu\nu;\alpha\beta}$ are parity even. From helicity analysis it is known that the decay of a massive spin-2 particle to two identical, massive, spin-1 particles is described by six helicity amplitudes. Bose symmetry between the pair of Z bosons [67,68] imposes constraints on the vertex $V_{HZZ}^{\mu\nu;\alpha\beta}$ such that it gets contributions from two parity-odd terms that are the admixture of one $\mathcal{P}$-wave and one $\mathcal{F}$-wave, and four parity-even terms that are some combinations of one $\mathcal{S}$-wave, two $\mathcal{D}$-waves and one $\mathcal{G}$-wave contributions. Even for the case of spin-2 boson we choose to work with helicity amplitudes as they are orthogonal but choose a basis such that amplitudes have definite parity associated with them. We find the following six helicity amplitudes in the transversity basis:

$$A_L = \frac{4X}{3\mathsf{u}_1}(E(\mathsf{u}_2^4 - M_H^2\mathsf{u}_1^2) + F(4\mathsf{u}_1^2M_H^2X^2)), \tag{40}$$

$$A_M = \frac{8\sqrt{q_1^2q_2^2}\mathsf{v}X}{3\sqrt{3}\mathsf{u}_1}E, \tag{41}$$

$$\begin{aligned} A_1 = \frac{2\sqrt{2}}{3\sqrt{3}M_H^2}&(A(M_H^4 - \mathsf{u}_2^4) - B(8M_H^4X^2) \\ &+ C(4M_H^2X^2)(\mathsf{u}_1^2 - M_H^2) - D(8M_H^4X^4)), \end{aligned} \tag{42}$$

$$A_2 = \frac{8\sqrt{q_1^2q_2^2}}{3\sqrt{3}}(A + 4X^2C), \tag{43}$$

$$A_3 = \frac{4}{3M_H\mathsf{u}_1}(A(\mathsf{u}_2^4 - M_H^2\mathsf{u}_1^2) + B(4\mathsf{u}_1^2M_H^2X^2)), \tag{44}$$

$$A_4 = \frac{8\sqrt{q_1^2q_2^2}\mathsf{w}}{3M_H\mathsf{u}_1}A, \tag{45}$$

where u_1, u_2, v and w are defined as

$$\mathsf{u}_1^2 = q_1^2 + q_2^2, \tag{46}$$

$$\mathsf{u}_2^2 = q_1^2 - q_2^2, \tag{47}$$

$$\mathsf{v}^2 = 4M_H^2\mathsf{u}_1^2 + 3\mathsf{u}_2^4, \tag{48}$$

$$\mathsf{w}^2 = 2M_H^2\mathsf{u}_1^2 + \mathsf{u}_2^4. \tag{49}$$

The quantity X is as defined in Eq. (5).

We wish to clarify that our vertex factor $V_{HZZ}^{\mu\nu;\alpha\beta}$ is the most general one. An astute reader can easily write down terms that are not included in our vertex and wonder how such a conclusion of generality can be made. For example, one can add a new possible term such as $iG(\epsilon^{\alpha\beta\nu\rho}P_\rho Q^\mu + \epsilon^{\alpha\beta\mu\rho}P_\rho Q^\nu)$. It is easy to verify that this new form factor G enters our helicity amplitudes A_L and A_M in the combination $(E - 2G)$:

$$A_L = \frac{4X}{3\mathsf{u}_1}((E - 2G)(\mathsf{u}_2^4 - M_H^2\mathsf{u}_1^2) + F(4\mathsf{u}_1^2M_H^2X^2)), \tag{50}$$

$$A_M = \frac{8\sqrt{q_1^2q_2^2}\mathsf{v}X}{3\sqrt{3}\mathsf{u}_1}(E - 2G). \tag{51}$$

Note that only this combination of E and G is accessible to experiments and all other helicity amplitudes remain unchanged. Since, there exist only six independent helicity amplitudes corresponding to six partial waves for the spin-2 case, the number of helicity amplitudes in the transversity basis must also be six. Adding any new terms to the vertex factor will simply modify the expressions for the helicity amplitudes. The generality of our vertex $V_{HZZ}^{\mu\nu;\alpha\beta}$ is therefore

very robust. Having established the generality of $V_{HZZ}^{\mu\nu;\alpha\beta}$ we will henceforth not consider any term absent in the vertex of Eq. (39). Our helicity amplitudes are different from those given in Ref. [66]. In Ref. [66], they provide eight independent helicity amplitudes. If we consider the Bose symmetry of the two identical vector bosons to which H is decaying, then these should reduce to six independent helicity amplitudes. Again as stated in the scalar case, our helicity amplitudes are classified by their parity and thus differ from those in Ref. [66]. Our amplitudes A_L and A_M have parity-odd behavior, and the rest of the helicity amplitudes have parity-even behavior. In contrast not all the amplitudes enunciated in Ref. [66] have clear parity characteristics.

Once again just as in the scalar case we will start by assuming that Z_1 is on-shell while Z_2 is off-shell. The integration over q_1^2 is done using the narrow width approximation of the Z. In tensor case, however, off-shell Z_1 will also have to be considered in a special case. We hence consider that q_1^2 is explicitly integrated out whether Z_1 is off-shell or fully on-shell. In case Z_1 is off-shell the resulting helicities are some weighted averaged values and should not be confused with well defined values at $q_1^2 \equiv M_Z^2$. The differential decay rate for the process $H \to Z_1 + Z_2^* \to (\ell_1^- + \ell_1^+) + (\ell_2^- + \ell_2^+)$, after integrating over q_1^2 (assuming Z_1 is on-shell or even otherwise) can now be written in terms of the angular distribution using the vertex given in Eq. (39) as

$$
\begin{aligned}
\frac{8\pi}{\Gamma_f}\frac{d^4\Gamma}{dq_2^2 d\cos\theta_1 d\cos\theta_2 d\phi} &= 1 + \left(\frac{1}{4}|F_2|^2 - \left(M_H^2\frac{u_1^2}{v^2}\right)|F_M|^2\right)\cos 2\phi(1-P_2(\cos\theta_1))(1-P_2(\cos\theta_2)) \\
&+ \left(M_H\frac{u_1}{v}\right)\mathrm{Im}(F_2F_M^*)\sin 2\phi(1-P_2(\cos\theta_1))(1-P_2(\cos\theta_2)) \\
&+ \frac{P_2(\cos\theta_1)}{2}\left((-2|F_1|^2+|F_2|^2)+(|F_3|^2+|F_L|^2)\left(\frac{q_1^2-2q_2^2}{u_1^2}\right)\right. \\
&\left.+|F_M|^2\left(4M_H^2\frac{u_1^2}{v^2}+3\frac{u_2^4}{u_1^2v^2}(q_2^2-2q_1^2)\right)+|F_4|^2\left(2M_H^2\frac{u_1^2}{w^2}+\frac{u_2^4}{u_1^2w^2}(q_2^2-2q_1^2)\right)\right. \\
&\left.+\left(6\sqrt{q_1^2q_2^2}\frac{u_2^2}{u_1^2w}\right)\mathrm{Re}(F_3F_4^*)+\left(6\sqrt{3}\sqrt{q_1^2q_2^2}\frac{u_2^2}{u_1^2v}\right)\mathrm{Re}(F_LF_M^*)\right) \\
&+ \frac{P_2(\cos\theta_2)}{2}\left((-2|F_1|^2+|F_2|^2)+(|F_3|^2+|F_L|^2)\left(\frac{q_2^2-2q_1^2}{u_1^2}\right)\right. \\
&\left.+|F_M|^2\left(4M_H^2\frac{u_1^2}{v^2}+3\frac{u_2^4}{u_1^2v^2}(q_1^2-2q_2^2)\right)+|F_4|^2\left(2M_H^2\frac{u_1^2}{w^2}+\frac{u_2^4}{u_1^2w^2}(q_1^2-2q_2^2)\right)\right. \\
&\left.-\left(6\sqrt{q_1^2q_2^2}\frac{u_2^2}{u_1^2w}\right)\mathrm{Re}(F_3F_4^*)-\left(6\sqrt{3}\sqrt{q_1^2q_2^2}\frac{u_2^2}{u_1^2v}\right)\mathrm{Re}(F_LF_M^*)\right) \\
&+ \frac{P_2(\cos\theta_1)P_2(\cos\theta_2)}{2}\left(2|F_1|^2+\frac{1}{2}|F_2|^2-|F_3|^2-|F_L|^2-\left(\frac{u_2^4-M_H^2u_1^2}{w^2}\right)|F_4|^2\right. \\
&\left.+\left(\frac{2M_H^2u_1^2-3u_2^4}{v^2}\right)|F_M|^2\right)+\frac{9\sin 2\theta_1\sin 2\theta_2\cos\phi}{16}\left((|F_3|^2-|F_L|^2)\left(\frac{\sqrt{q_1^2q_2^2}}{u_1^2}\right)\right. \\
&\left.+3|F_M|^2\left(\sqrt{q_1^2q_2^2}\frac{u_2^4}{u_1^2v^2}\right)-|F_4|^2\left(\sqrt{q_1^2q_2^2}\frac{u_2^4}{u_1^2w^2}\right)-\left(\frac{u_2^4}{u_1^2w}\right)\mathrm{Re}(F_3F_4^*)\right. \\
&\left.+\left(\sqrt{3}\frac{u_2^4}{u_1^2v}\right)\mathrm{Re}(F_LF_M^*)-\sqrt{2}\mathrm{Re}(F_1F_2^*)\right)+\frac{9\sin 2\theta_1\sin 2\theta_2\sin\phi}{16}\left(\left(2\frac{\sqrt{q_1^2q_2^2}}{u_1^2}\right)\mathrm{Im}(F_3F_L^*)\right. \\
&\left.-\left(\sqrt{3}\frac{u_2^4}{u_1^2v}\right)\mathrm{Im}(F_3F_M^*)-\left(\frac{u_2^4}{u_1^2w}\right)\mathrm{Im}(F_4F_L^*)-\left(2\sqrt{3}\sqrt{q_1^2q_2^2}\frac{u_2^4}{u_1^2vw}\right)\mathrm{Im}(F_4F_M^*)\right. \\
&\left.-\left(2\sqrt{2}M_H\frac{u_1}{v}\right)\mathrm{Im}(F_1F_M^*)\right)+\mathcal{M}, \qquad (52)
\end{aligned}
$$

where $\mathcal{M}$ includes all the terms that are proportional to η and η^2, and is written explicitly in the Appendix, Eq. (A1). The helicity fractions are defined as

$$F_i = \frac{A_i}{\sqrt{\sum_j |A_j|^2}}, \tag{53}$$

and Γ_f is given by

$$\Gamma_f \equiv \frac{d\Gamma}{dq_2^2} = \frac{1}{5}\frac{9}{2^{10}}\frac{1}{\pi^3} X \frac{\mathrm{Br}^2_{\ell\ell}}{M_H^2}\frac{\Gamma_Z}{M_Z^3}\frac{\sum_j |A_j|^2}{((q_2^2 - M_Z^2)^2 + M_Z^2\Gamma_Z^2)}, \tag{54}$$

where $i, j \in \{L, M, 1, 2, 3, 4\}$ and we have averaged over the 5 initial polarization states of the spin-2 boson.

The uniangular distributions are given by

$$\frac{1}{\Gamma_f}\frac{d^2\Gamma}{dq_2^2 d\cos\theta_1} = \frac{1}{2} + T_2^{(2)} P_2(\cos\theta_1) - T_1^{(2)}\cos\theta_1, \tag{55}$$

$$\frac{1}{\Gamma_f}\frac{d^2\Gamma}{dq_2^2 d\cos\theta_2} = \frac{1}{2} + T_2'^{(2)} P_2(\cos\theta_2) + T_1'^{(2)}\cos\theta_2, \tag{56}$$

$$\frac{2\pi}{\Gamma_f}\frac{d^2\Gamma}{dq_2^2 d\phi} = 1 + U_2^{(2)}\cos 2\phi + V_2^{(2)}\sin 2\phi + U_1^{(2)}\cos\phi + V_1^{(2)}\sin\phi, \tag{57}$$

where the superscript (2) is used to denote the fact that the concerned coefficients are for spin-2 resonance, and

$$T_2^{(2)} = \frac{1}{4}\Bigg(-2|F_1|^2 + |F_2|^2 + (|F_3|^2 + |F_L|^2)\left(\frac{q_1^2 - 2q_2^2}{\mathsf{u}_1^2}\right) + |F_4|^2\left(2M_H^2\frac{\mathsf{u}_1^2}{\mathsf{w}^2} + \frac{\mathsf{u}_2^4}{\mathsf{u}_1^2\mathsf{w}^2}(q_2^2 - 2q_1^2)\right) + |F_M|^2\left(4M_H^2\frac{\mathsf{u}_1^2}{\mathsf{v}^2} + 3\frac{\mathsf{u}_2^4}{\mathsf{u}_1^2\mathsf{v}^2}(q_2^2 - 2q_1^2)\right) + 6\sqrt{q_1^2 q_2^2}\frac{\mathsf{u}_2^2}{\mathsf{u}_1^2\mathsf{v}\mathsf{w}}(\mathsf{v}\mathrm{Re}(F_3F_4^*) + \sqrt{3}\mathsf{w}\mathrm{Re}(F_L F_M^*))\Bigg), \tag{58}$$

$$T_2'^{(2)} = \frac{1}{4}\Bigg(-2|F_1|^2 + |F_2|^2 + (|F_3|^2 + |F_L|^2)\left(\frac{q_2^2 - 2q_1^2}{\mathsf{u}_1^2}\right) + |F_4|^2\left(2M_H^2\frac{\mathsf{u}_1^2}{\mathsf{w}^2} + \frac{\mathsf{u}_2^4}{\mathsf{u}_1^2\mathsf{w}^2}(q_1^2 - 2q_2^2)\right) + |F_M|^2\left(4M_H^2\frac{\mathsf{u}_1^2}{\mathsf{v}^2} + 3\frac{\mathsf{u}_2^4}{\mathsf{u}_1^2\mathsf{v}^2}(q_1^2 - 2q_2^2)\right) - 6\sqrt{q_1^2 q_2^2}\frac{\mathsf{u}_2^2}{\mathsf{u}_1^2\mathsf{v}\mathsf{w}}(\mathsf{v}\mathrm{Re}(F_3F_4^*) + \sqrt{3}\mathsf{w}\mathrm{Re}(F_L F_M^*))\Bigg), \tag{59}$$

$$U_2^{(2)} = \frac{1}{4}|F_2|^2 - \frac{M_H^2\mathsf{u}_1^2}{\mathsf{v}^2}|F_M|^2, \tag{60}$$

$$V_2^{(2)} = M_H\frac{\mathsf{u}_1}{\mathsf{v}}\mathrm{Im}(F_2F_M^*), \tag{61}$$

$$T_1^{(2)} = \frac{3\eta}{2\mathsf{u}_1^2\mathsf{v}\mathsf{w}}\Big(2M_H\mathsf{u}_1^3\mathsf{w}\mathrm{Re}(F_2F_M^*) + q_1^2\mathsf{v}\mathsf{w}\mathrm{Re}(F_3F_L^*) + \sqrt{q_2^2}\mathsf{u}_2^2\Big(\sqrt{3}\sqrt{q_1^2}\mathsf{w}\mathrm{Re}(F_3F_M^*) + \sqrt{q_1^2}\mathsf{v}\mathrm{Re}(F_4F_L^*) + \sqrt{3}\sqrt{q_2^2}\mathsf{u}_2^2\mathrm{Re}(F_4F_M^*)\Big)\Big), \tag{62}$$

$$T_1'^{(2)} = \frac{3\eta}{2\mathsf{u}_1^2\mathsf{v}\mathsf{w}}\Big(2M_H\mathsf{u}_1^3\mathsf{w}\mathrm{Re}(F_2F_M^*) + q_2^2\mathsf{v}\mathsf{w}\mathrm{Re}(F_3F_L^*) + \sqrt{q_1^2}\mathsf{u}_2^2\Big(-\sqrt{3}\sqrt{q_2^2}\mathsf{w}\mathrm{Re}(F_3F_M^*) - \sqrt{q_2^2}\mathsf{v}\mathrm{Re}(F_4F_L^*) + \sqrt{3}\sqrt{q_1^2}\mathsf{u}_2^2\mathrm{Re}(F_4F_M^*)\Big)\Big), \tag{63}$$

$$U_1^{(2)} = \frac{9\pi^2\eta^2}{64\mathsf{u}_1^2\mathsf{v}^2\mathsf{w}^2}\Big(\sqrt{2}\mathsf{u}_1^2\mathsf{v}^2\mathsf{w}^2\mathrm{Re}(F_1F_2^*) - \mathsf{u}_2^4\mathsf{v}^2\mathsf{w}\mathrm{Re}(F_3F_4^*) + |F_3|^2\sqrt{q_1^2q_2^2}\mathsf{v}^2\mathsf{w}^2 - |F_4|^2\sqrt{q_1^2q_2^2}\mathsf{u}_2^4\mathsf{v}^2 + \sqrt{3}\mathsf{u}_2^4\mathsf{v}\mathsf{w}^2\mathrm{Re}(F_LF_M^*) - |F_L|^2\sqrt{q_1^2q_2^2}\mathsf{v}^2\mathsf{w}^2 + 3|F_M|^2\sqrt{q_1^2q_2^2}\mathsf{u}_2^4\mathsf{w}^2\Big), \tag{64}$$

$$V_1^{(2)} = \frac{9\pi^2\eta^2}{64\mathsf{u}_1^2\mathsf{v}\mathsf{w}}\Big(2\sqrt{2}M_H\mathsf{u}_1^3\mathsf{w}\mathrm{Im}(F_1F_M^*) + 2\sqrt{q_1^2q_2^2}\mathsf{v}\mathsf{w}\mathrm{Im}(F_3F_L^*) - \sqrt{3}\mathsf{u}_2^4\mathsf{w}\mathrm{Im}(F_3F_M^*) - \mathsf{u}_2^4\mathsf{v}\mathrm{Im}(F_4F_L^*) - 2\sqrt{3}\mathsf{u}_2^4\sqrt{q_1^2q_2^2}\mathrm{Im}(F_4F_M^*)\Big). \tag{65}$$

These coefficients can again be extracted from asymmetries similar to those defined in Eqs. (22), (23), (24), (25), (26) and (27) for the spin-0 case. We find that the angular distributions corresponding to $P_2(\cos\theta_1)$ and $P_2(\cos\theta_2)$ are different in the spin-2 case in contrast to the spin-0 case. This feature can enable us to distinguish between the two spins, unless the difference happens to be zero for certain choice of parameters, even in the spin-2 case. Considering only the η independent terms in Eqs. (55) and (56), the difference Δ between the coefficients of $P_2(\cos\theta_1)$ and $P_2(\cos\theta_2)$ in

$$\frac{1}{\Gamma_f}\frac{d^2\Gamma}{dq_2^2 d\cos\theta_1} \quad \text{and} \quad \frac{1}{\Gamma_f}\frac{d^2\Gamma}{dq_2^2 d\cos\theta_2}$$

respectively, is

$$\Delta = \frac{3\mathsf{u}_2^2}{4\mathsf{u}_1^2\mathsf{v}^2\mathsf{w}^2}(\mathsf{v}^2\mathsf{w}^2(|F_3|^2 + |F_L|^2) - \mathsf{u}_2^4(\mathsf{v}^2|F_4|^2 + 3\mathsf{w}^2|F_M|^2)) + \frac{3\sqrt{q_1^2q_2^2}\mathsf{u}_2^2}{\mathsf{u}_1^2\mathsf{v}\mathsf{w}}(\mathsf{v}\mathrm{Re}(F_3F_4^*) + \sqrt{3}\mathsf{w}\mathrm{Re}(F_LF_M^*)). \tag{66}$$

If we find that $\Delta = 0$ for all $\sqrt{q_2^2}$, then the tensor case would have similar characteristics in the uniangular distributions as discussed in the scalar case. However, this can only happen if

helicity amplitudes (or equivalently the corresponding coefficients A, B, C, D, E and F) have the explicit momentum dependence so as to absorb $\sqrt{q_2^2}$ completely in Δ. The reader can examine the expression for Δ to conclude that this is impossible and the only way Δ can be equated to zero for all $\sqrt{q_2^2}$, is when

$$F_3 = F_4 = F_L = F_M = 0. \tag{67}$$

In such a special case all the form factors in vertex $V_{HZZ}^{\mu\nu;\alpha\beta}$ vanish, except C and D. This special case explicitly implies that the parity of the spin-2 boson is even. We will refer to this case as the special $J^P = 2^+$ case, since the uniangular distribution mimics the $J^P = 0^+$ case. Working under this special case

$$\frac{1}{\Gamma_f}\frac{d^2\Gamma}{dq_2^2 d\cos\theta_1} = \frac{1}{2} + T_2^{(2)} P_2(\cos\theta_1), \tag{68}$$

$$\frac{1}{\Gamma_f}\frac{d^2\Gamma}{dq_2^2 d\cos\theta_2} = \frac{1}{2} + T_2^{(2)} P_2(\cos\theta_2), \tag{69}$$

$$\frac{2\pi}{\Gamma_f}\frac{d^2\Gamma}{dq_2^2 d\phi} = 1 + U_2^{(2)}\cos 2\phi + U_1^{(2)}\cos\phi, \tag{70}$$

where the $T_2^{(2)}$, $U_2^{(2)}$ and $U_1^{(2)}$ are now given by

$$T_2^{(2)} = \frac{1}{4}(|F_2|^2 - 2|F_1|^2), \tag{71}$$

$$U_2^{(2)} = \frac{1}{4}|F_2|^2, \tag{72}$$

$$U_1^{(2)} = \frac{9\pi^2}{32\sqrt{2}}\eta^2 \mathrm{Re}(F_1 F_2^*). \tag{73}$$

Now using the identity $|F_1|^2 + |F_2|^2 = 1$, we get

$$U_2^{(2)} = \frac{1}{6}(1 + 2T_2^{(2)}). \tag{74}$$

Note the similarity between Eqs. (33) and (74). The conclusions that $J^P = 2^\pm$ when $\Delta \neq 0$ can also be drawn if Δ integrated over q_1^2 and q_2^2 is found to be nonzero. However, it is clear from Eq. (66) that the domain of integration for q_1^2 and q_2^2 cannot be symmetric.

C. Comparison between spin-0 and spin-2

Having discussed both the scalar and tensor cases, we summarize the procedure to distinguish the spin and parity states of the new boson in a flowchart in Fig. 3. The procedure entailed ensures that we convincingly determine the spin and parity of the boson. The first step should be to compare the uniangular distributions in $\cos\theta_1$ and $\cos\theta_2$. If the distribution is found to be different the boson cannot be the SM Higgs and indeed must have spin-2. However, if the distributions are found to be identical the resonance can have spin-0 or be a very special case of spin-2 arising only from C and D terms in the vertex in Eq. (39). The similarity between Eqs. (33) and (74) makes it impossible to distinguish these two cases by looking at angular distributions alone.

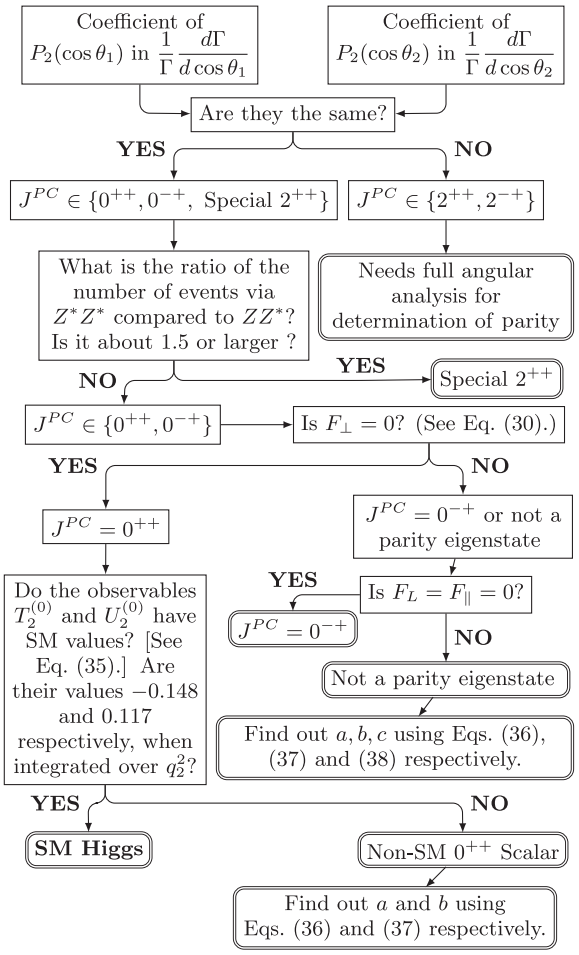

FIG. 3. Flow chart for determination of spin and parity of the new boson. See text for details.

The special $J^P = 2^+$ case can nevertheless still be identified by examining the surviving helicity amplitudes A_1 and A_2. The helicity amplitudes given in Eqs. (42) and (43) reduce in this special case to

$$A_1 = -\frac{16\sqrt{2}}{3\sqrt{3}} X^2 (q_1.q_2 C + M_H^2 X^2 D), \tag{75}$$

$$A_2 = \frac{32}{3\sqrt{3}}\sqrt{q_1^2 q_2^2} X^2 C. \tag{76}$$

These may be compared with Eqs. (2) and (3) to notice that they have identical form, except for an additional X^2 dependence in A_1 and A_2 expressions above. The additional X^2 dependence increases the contribution from both off-shell Z's (called Z^*Z^*) significantly in comparison to the

dominant one on-shell and one off-shell Z (called ZZ^*) contribution expected in SM. In the SM one would expect the ratio of the number of events in Z^*Z^* to ZZ^* channel to be about 0.2. However, in the special $J^P = 2^+$ case we would expect this ratio to be about 1.5. The reader is cautioned not to confuse this explicit X^2 dependence with any assumption on the momentum dependence of the form factors. Throughout the analysis we have assumed the most general form factors a, b, c, A, B, C, D, E and F; nevertheless A_1 and A_2 turn out to have additional X^2 dependence in comparison to A_L and $A_\parallel$ respectively. This explicit X^2 dependence arises due to contributions only from higher dimensional operators in the special $J^P = 2^+$ case.

Having excluded the spin-2 possibility, the resonance would be a parity-odd state (0^{-+}) if $F_L = F_\parallel = 0$ and a parity-even state (0^{++}) if $F_\perp = 0$. If the resonance is found to be in 0^{++} state, we need to check whether $T_2^{(0)}$ and $U_2^{(0)}$ terms are as predicted in SM. The values of $T_2^{(0)}$ and $U_2^{(0)}$ as a function of $\sqrt{q_2^2}$ are plotted in Fig. 2. The q_2^2 integrated values for the observables $T_2^{(0)}$ and $U_2^{(0)}$ are uniquely predicted in SM at tree level to be -0.148 and 0.117 respectively. These tests would ascertain whether the 0^{++} state is the SM Higgs or some non-SM boson. If it turns out to be a non-SM boson, we can also measure the coefficients a, b, c by using Eqs. (36), (37) and (38).

Finally we emphasize that our approach is unique in using helicity amplitudes in the transversity basis so that the amplitudes are classified by parity. We also use the orthogonality of Legendre polynomials in $\cos\theta_1$ and $\cos\theta_2$ as well as a Fourier series in ϕ to unambiguously determine the spin and parity of the new resonance. Another significant achievement is the use of the most general HZZ vertex factors for both spin-0 and spin-2 cases allowing us to determine the nature of H be it in any extension of the SM. We wish to stress that we consider neither any specific mode of production of the new resonance (like gluon-gluon fusion or vector boson fusion), nor any specific model for its couplings. The production channel for the new resonance has no role in our analysis. We consider its decay only to four leptons via two Z bosons. Most discussions in current literature deal either with specific production channels or with specific models of new physics which restrict the couplings to specific cases both for spin-0 and spin-2. References [34,37,38,45,46] deal with gravitonlike spin-2 particles, while Ref. [47] deals with spin-2 states that are singlet or triplet under $SU(2)$. Reference [34] considers polar angle distribution of $\gamma\gamma$ and angular correlations between the charged leptons coming from WW^* decays to differentiate between the spin-0 and spin-2 possibilities. While Ref. [37] looks at Higgs-strahlung process to distinguish the various spin and parity possibilities, Ref. [38] compares branching ratios of the new boson decaying to $\gamma\gamma$, WW^* and ZZ^* channels as a method to measure the spin and parity of the new boson. In Ref. [45] the authors propose a new observable that can distinguish SM Higgs from a spin-2 possibility. They consider the three-body decay of the new resonance to a SM vector boson and a fermion-antifermion pair. Reference [46] shows that the current data disfavors a particular type of gravitonlike spin-2 particle that appears in scenarios with a warped extra dimension of the anti–de-Sitter type. References [47,48] deal with spin-0 or spin-2 particles produced via vector boson fusion process alone. Our discussion subsumes all of the above special cases. Moreover, unlike other discussions in the literature we provide clearly laid out steps to measure the couplings, spin and parity of the new resonance H without any ambiguity. We want to reiterate that it is important to measure not only the spin and parity of the new resonance but also its couplings before any conclusive statements can be made that it is the SM Higgs.

D. Numerical study of the uniangular distributions

In this subsection we study the possibility of using the uniangular distributions, given in previous subsection to differentiate the different possible spin CP states. For simplicity throughout this subsection we will neglect the q^2 dependence of a, b and c. The signal and background events were generated using the MadEvent5 [69] event generator interfaced with PYTHIA 6.4 [70] and PGS 4 [71]. The vertex of Eq. (1) was implemented into the UFO format of Madgraph5 using Feynrules 1.6.18 [72]. Unlike the earlier subsections we also include the $2e^+2e^-$ and $2\mu^+2\mu^-$ final states because the identification of Z_1 being the mother particle of the pair of same flavor opposite sign leptons with an invariant mass closest to the M_Z breaks the exchange symmetry of these final states in most regions of phase space. As the analysis of this paper has to do purely with the shape of the partial widths in the $Z^{(*)}Z^{(*)}$ channel, the production mechanism is not crucial to understanding the spin and CP properties of the resonance at 125 GeV. However to be concrete, these samples were generated for pp collisions at $\sqrt{s} = 8$ TeV using the CTEQ6L1 parton distribution functions [73]. We choose to follow the ATLAS cut based analysis of Ref. [74] instead of the CMS analysis [65] because the CMS analysis has used a more sophisticated multivariate analysis technique. We set the Higgs boson mass $m_H = 125$ GeV, which is close to what has been measured in Ref. [74]. The branching ratios and decay widths are set appropriately using the values from the Higgs working group webpage [75].

Following the analysis of Ref. [74] we impose the following lepton selection cuts and triggers. In particular, the single lepton trigger thresholds are $p_T^l > 24(25)$ GeV for a muon(electron). The dimuon trigger thresholds used are $p_T > 13$ GeV for the symmetric case and $p_T^1 > 18$ GeV and $p_T^2 > 8$ GeV for the asymmetric case. For dielectrons the thresholds are $p_T > 12$ GeV. The lepton identification cuts require that each electron(muon) must have $E_T > 7$ GeV ($p_T > 6$ GeV) with $|\eta| < 2.4(2.7)$. Sorting leptons in decreasing order of p_T, we also impose

the selection criteria $p_T^{\ell_1} > 20$ GeV, $p_T^{\ell 2} > 15$ GeV and $p_T^{\ell_3} > 10$ GeV. For same flavor leptons we also require that $\Delta R > 0.1$ while for opposite flavor $\Delta R > 0.2$. Furthermore we also impose the invariant mass cuts on the m_{Z_1}, m_{Z_2} and $m_{4\ell}$ described in Table I to reduce the Standard Model background. m_{Z_1} is the invariant mass of the pair of opposite sign same flavor leptons closest to m_Z while m_{Z_2} is the other combination. The number of signal events in our simulation is in good agreement with the SM predicted value quoted in Ref. [74], while the background rate is slightly lower than total background rate because we have not included the subdominant processes like $Z +$ jets and $t\bar{t}$.

In order to quantify the effect of using the uniangular distributions to extract the nature of the 125 GeV resonance we construct the test statistic q based on the ratio of the likelihoods

$$q = \ln \frac{\mathcal{L}_{0^+}}{\mathcal{L}_{0^-}}, \tag{77}$$

where the $\mathcal{L}$ is the unbinned likelihood function

$$\mathcal{L} = \sum_{\mu_s} \left(\prod_i^{N_{\rm obs}} \frac{\mu_s P_s(\mathbf{x}_i) + \mu_b P_b(\mathbf{x}_i)}{\mu_s + \mu_b} \right)_{\rm ave}. \tag{78}$$

As our acceptances are in good agreement with the ATLAS predictions for the rest of our analysis we will assume a background rate $\mu_b = 16$ events for luminosity $L = 20.7$ fb^{-1} due to the continuum ZZ background. However as the total observed number of events are slightly above the expected rate we need to marginalize over the expected signal rate. In particular

TABLE I. Effect of the sequential cuts on the simulated Signal and the dominant continuum ZZ background, where the k factors are 1.3 for signal and 2.2 for background using MCFM 6.6 [76] for 20.7 fb^{-1}.

Cuts	$m_H = 125$ GeV	SM ZZ^*
Selection	22	1542
50 GeV $< m_{Z_1} <$ 106 GeV	20	1432
12 GeV $< m_{Z_2} <$ 115 GeV	19	1294
115 GeV $< m_{4\ell} <$ 130 GeV	19	14

we assume a Bayesian prior flat distribution for $\mu_s \in [0.5, 2.0] \times \mu_s^{\rm SM} (= 18$ at a luminosity of 20.7 fb$^{-1})$. For a particular value of μ_s we generate ensembles of $N_{\rm obs}$ events to find the average of the product within the brackets in Eq. (78). The probability density function for signal is the product of the distributions

$$\frac{1}{\Gamma}\frac{d\Gamma}{d\cos\theta_1} = \frac{1}{2} - \mathcal{T}_1^{(0)}(a,B,C)\cos\theta_1 + \mathcal{T}_2^{(0)}(a,B,C)P_2(\cos\theta_1), \tag{79}$$

$$\frac{1}{\Gamma}\frac{d\Gamma}{d\cos\theta_2} = \frac{1}{2} + \mathcal{T}_1^{(0)}(a,B,C)\cos\theta_2 + \mathcal{T}_2^{(0)}(a,B,C)P_2(\cos\theta_2), \tag{80}$$

$$\frac{1}{\Gamma}\frac{d\Gamma}{d\phi} = \frac{1}{2\pi} + \mathcal{U}_1^{(0)}(a,B,C)\cos\phi + \mathcal{U}_2^{(0)}(a,B,C)\cos 2\phi, \tag{81}$$

where $B = b \times (100\ \text{GeV})^2$, $C = c \times (100\ \text{GeV})^2$ and

$$\Gamma \equiv \Gamma(a,B,C) \simeq 2.24 \times 10^{-8} x_H^{14} (a^2 + 0.19aB + 2.22 \times 10^{-2} B^2 x_H^2 + 2.14 \times 10^{-2} C^2 x_H^6), \tag{82}$$

$$\mathcal{T}_1^{(0)}(a,B,C) \simeq \frac{2.14 \times 10^{-2} a C x_H^3}{a^2 + 0.19aB + 2.22 \times 10^{-2} B^2 x_H^2 + 2.14 \times 10^{-2} C^2 x_H^6}, \tag{83}$$

$$\mathcal{T}_2^{(0)}(a,B,C) \simeq \frac{-0.15a^2 - 9.65 \times 10^{-2} aB x_H^3 + 5.35 \times 10^{-3} C^2 x_H^9}{x_H^3 (a^2 + 0.19aB + 2.22 \times 10^{-2} B^2 x_H^2 + 2.14 \times 10^{-2} C^2 x_H^6)}, \tag{84}$$

$$\mathcal{U}_1^{(0)}(a,B,C) \simeq \frac{-3.44 \times 10^{-3} a^2 - 5.50 \times 10^{-4} aB x_H^2}{a^2 + 0.19aB + 2.22 \times 10^{-2} B^2 x_H^2 + 2.14 \times 10^{-2} C^2 x_H^6}, \tag{85}$$

$$\mathcal{U}_2^{(0)}(a,B,C) \simeq \frac{1.88 \times 10^{-2} a^2 x_H - 8.51 \times 10^{-4} C^2 x_H^6}{a^2 + 0.19aB + 2.22 \times 10^{-2} B^2 x_H^2 + 2.14 \times 10^{-2} C^2 x_H^6}, \tag{86}$$

while for the background $P_b = 1/(8\pi)$. In the above approximations for the observables we have neglected the q^2 dependences of a, b and c and integrated Eq. (9), Eq. (13), Eq. (14) and Eq. (15) over q_2^2. Furthermore we have performed a power law fit in terms of $x_H = m_H/(120\ \text{GeV})$ for each of the coefficients. As b and c have dimensions of mass squared, in the above approximations for the different coefficients we have used the dimensionless coefficients B and C instead. By definition, the 0^+ hypothesis corresponds to

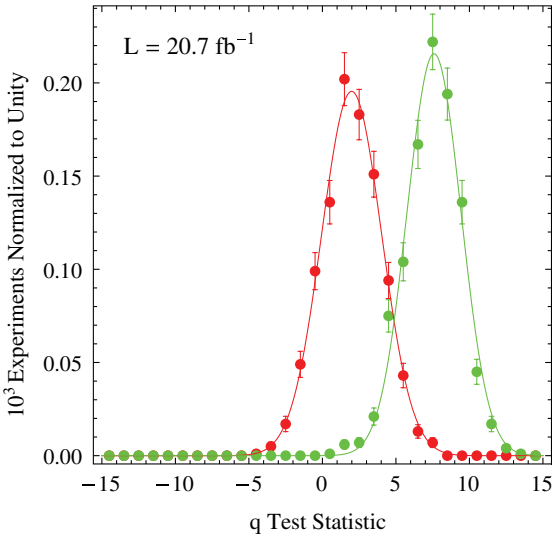

FIG. 4 (color online). Comparison of the q-test statistic using the uniangular distribution approach in the 4ℓ channel for the 0^+ events in red (gray) vs. 0^- events in green (light gray).

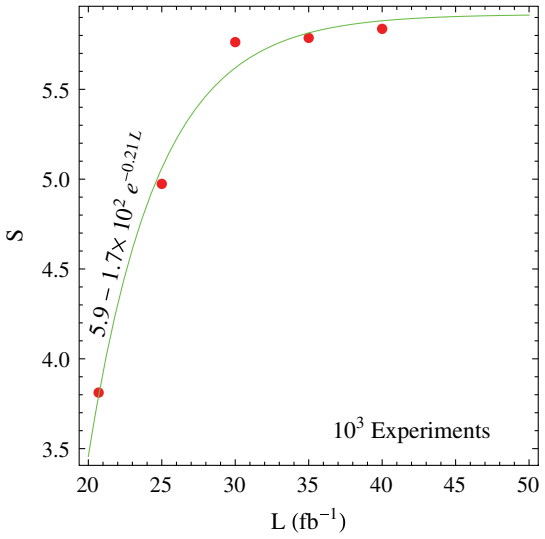

FIG. 5 (color online). Separation power for q-test statistic using the uniangular distributions as a function of luminosity. The red (dark grey) points are the simulated separation power and the green (light grey) curve is the fit to the data.

$(a, B, C) = (1, 0, 0)$ and the 0^- hypothesis corresponds to $(a, B, C) = (0, 0, 1)$. When $a = 0$ the magnitude of C is not crucial as we normalize the 0^+ and 0^- cross sections so as to produce the same number of signal events.

To quantify power of the uniangular distributions in hypothesis testing, we present the q-test statistic for the 0^+ and 0^- hypotheses in Fig. 4. In particular, we have applied the q statistic in Eq. (77) to samples of Monte Carlo events that have passed the above cuts in Table I, where we assumed the above Bayesian prior for the mean signal rate. The red (dark grey) curve corresponds to 0^- events while the green (light grey) curve corresponds to 0^+ events. The solid curves correspond to a Gaussian fit to these distributions and using them we define the separation power as

$$S = \frac{2A}{\sigma}, \tag{87}$$

where A is the area under the curve calculated from the point on the q axis which satisfies the condition that the area under the right tail of the left distribution is equal to the left tail of the right distribution and σ is the maximum of the two standard deviations.

The separation power using the q-test statistic works well for low luminosity, but this approach loses sensitivity at larger luminosity. To illustrate this point we present in Fig. 5 the separation power S as a function of luminosity. The red (dark grey) points correspond to calculated separation power for a particular luminosity while the green (light grey) curve is a fit to the data. The lowest data point corresponds to a luminosity of 20.7 fb^{-1} with an observation of 43 events while for higher luminosities we have assumed that the number of observed events agrees with the expected rates. Furthermore this extrapolation assumes the same cuts and efficiencies for higher luminosities. For luminosities greater that 40 fb^{-1}, a χ^2 fit of the uniangular distributions would probably provide a stronger hypothesis test.

It would seem that the values of all the form factors a, b and c can be extracted using the three uniangular distributions given in Eqs. (79)–(81) along with Eqs. (82)–(86). However, the difference between the uniangular distributions in Eq. (79) and Eq. (80) is small because it is proportional to η. Given the small sample of 43 events this would essentially imply that only two parameters can be obtained. Our numerical work confirms this fact. Since $P_0(\cos\theta_{1,2}) = 1$, $P_1(\cos\theta_{1,2})$, $P_2(\cos\theta_{1,2})$, $\cos\phi$ and $\cos 2\phi$ are orthogonal functions the coefficients of each of the terms can be extracted individually. As discussed in Sec. II A this would result in four observables. We emphasize that as the data sample increases the additional information can be used to measure relative phases between a, b and c. For 43 events, as expected from the discussions in Sec. II A based on the small value of η in SM, we find we could only extract stable values of b/a and c/a by maximizing the likelihood function $\mathcal{L}_{0^+}$. One can also estimate the errors in b/a and c/a from the inverse of the covariance matrix $V_{ij} = \mathrm{cov}[\theta_i, \theta_j]$ defined as

$$\hat{V}^{-1} = -\left(\frac{\partial^2 \ln \mathcal{L}}{\partial\theta_i \partial\theta_j}\right)_{\hat{\theta}} \tag{88}$$

where $\theta_i, \theta_j = b/a, c/a$. Here $\hat{\theta}$ denotes those values of the parameters that maximizes the likelihood function. In Fig. 6 we present the extracted values of b/a and c/a for a sample of 43 events. Using these values of b/a and c/a, the value of a can also be found by fitting the decay

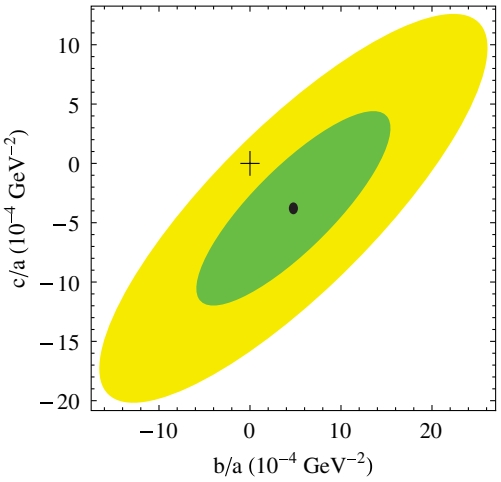

FIG. 6 (color online). c/a vs. b/a 1σ (green) and 2σ (yellow) contours assuming the Standard Model value of the partial decay width to 4ℓ. The central values $(b/a, c/a) = (4.77 \pm 21.23, -3.79 \pm 16.4) \times 10^{-4}\,\mathrm{GeV}^{-2}$ are shown by the block dot. The cross hair corresponds to $b = c = 0$.

width in Eq. (82) to the Standard Model partial width. Using this approach, the values of a, b and c with their respective errors are

$$a = 2.11 \pm 3.55, \tag{89}$$

$$b = (10.09 \pm 47.99) \times 10^{-4}\ \mathrm{GeV}^{-2}, \tag{90}$$

$$c = -(8.01 \pm 37.20) \times 10^{-4}\ \mathrm{GeV}^{-2}. \tag{91}$$

III. CONCLUSION

We conclude that by looking at the three uniangular distributions and examining the numbers of Z^*Z^* to ZZ^* events one can unambiguously confirm whether the new boson is indeed the Higgs with $J^{PC} = 0^{++}$ and with couplings to Z bosons exactly as predicted in the Standard Model. We show that the terms in the angular distribution corresponding to $P_2(\cos\theta_1)$ and $P_2(\cos\theta_2)$ play a critical role in distinguishing the $J = 2$ and $J = 0$ states. The distributions are identical for spin-0 case, but must be different for spin-2 state except in a special $J^P = 2^+$ case where $F_3 = F_4 = F_L = F_M = 0$. The ratio of the number of Z^*Z^* events to the number of ZZ^* events provides a unique identification for this special $J^P = 2^+$ case. In this special case the number of Z^*Z^* events dominates significantly over the number of ZZ^* events. The spin-2 resonance can thus be unambiguously confirmed or ruled out. With spin-2 possibility ruled out, spin-0 can be studied in detail.

The resonance would then be a parity-odd state (0^{-+}) if $F_L = F_\parallel = 0$ and a parity-even state (0^{++}) if $F_\perp = 0$. If the resonance is found to be in 0^{++} state, we need to check whether $T_2^{(0)}$ and $U_2^{(0)}$ terms are as predicted in SM. The q_2^2 integrated values for the observables $T_2^{(0)}$ and $U_2^{(0)}$ are uniquely predicted in SM at tree level to be -0.148 and 0.117 respectively. These tests would ascertain whether the 0^{++} state is the SM Higgs or some non-SM boson. If it turns out to be a non-SM boson, we can also measure the coefficients a, b, c by using Eqs. (36), (37) and (38). If the boson is a mixed parity state, the relative phase between the parity-even and parity-odd amplitudes can also be measured by studying the $\sin 2\phi$ term in the uniangular distribution. We present a step by step methodology in Fig. 3 for a quick and sure-footed determination of spin and parity of the newly discovered boson. Our approach of using Legendre polynomials and the choice of helicity amplitudes classified by parity enable us to construct angular asymmetries that unambiguously determine if the new resonance is indeed the Standard Model Higgs.

Numerically we have simulated the dominant continuum ZZ background and Standard Model signal for Higgs. It is shown that our acceptances are in good agreement with the ATLAS predictions. Using the uniangular distributions derived in this paper we compute the q statistic $q = \ln(\mathcal{L}_{0^+}/\mathcal{L}_{0^-})$. We observe the separation power of this approach is most powerful at low luminosity assuming that the cuts and the acceptances remain the same at each luminosity. For easy experimental adaption we have included power law parametrization of the various angular coefficients in terms of the fundamental Higgs vertex parameters. We also obtain fits for b/a and c/a for a 43-event sample, demonstrating that both b and c can be constrained by a rather small sample of data.

ACKNOWLEDGMENTS

R. S. is grateful to Institute of Physics, Academia Sinica, for hospitality where part of the work was done. We thank Sridhara Dasu for discussions. A. M. is supported by the U.S. Department of Energy under Contract No. DE-FG02-96ER40969.

APPENDIX: OTHER TERMS IN THE ANGULAR DISTRIBUTIONS

In the main text, we have not included the η and η^2 dependent term in the angular distributions for the case of spin-2 boson. However, for the sake of completeness, the η and η^2 dependent term $\mathcal{M}$ in the angular distributions are given below.

$$
\begin{aligned}
\mathcal{M} = \eta\Bigg(& -3M_H \mathrm{Re}(F_2 F_M^*)\frac{\mathsf{u}_1}{\mathsf{v}}(\cos\theta_1(P_2(\cos\theta_2)+2)-\cos\theta_2(P_2(\cos\theta_1)+2)) \\
& -\frac{3}{\mathsf{u}_1^2}\mathrm{Re}(F_3 F_L^*)(q_1^2\cos\theta_1(1-P_2(\cos\theta_2))-q_2^2\cos\theta_2(1-P_2(\cos\theta_1))) \\
& -3\sqrt{3}\sqrt{q_1^2 q_2^2}\mathrm{Re}(F_3 F_M^*)\frac{\mathsf{u}_2^2}{\mathsf{u}_1^2\mathsf{v}}(\cos\theta_1(1-P_2(\cos\theta_2))+\cos\theta_2(1-P_2(\cos\theta_1))) \\
& -3\sqrt{q_1^2 q_2^2}\mathrm{Re}(F_4 F_L^*)\frac{\mathsf{u}_2^2}{\mathsf{u}_1^2\mathsf{w}}(\cos\theta_1(1-P_2(\cos\theta_2))+\cos\theta_2(1-P_2(\cos\theta_1))) \\
& +12\sqrt{3}\mathsf{u}_2^4\mathrm{Re}(F_4 F_M^*)\frac{1}{4\mathsf{u}_1^2\mathsf{v}^3\mathsf{w}^3}(-q_2^2\mathsf{v}^2\mathsf{w}^2\cos\theta_1(1-P_2(\cos\theta_2)) \\
& +q_1^2\cos\theta_2(\mathsf{v}^2\mathsf{w}^2-P_2(\cos\theta_1)(8M_H^4\mathsf{u}_1^4+10M_H^2\mathsf{u}_1^2\mathsf{u}_2^4+3\mathsf{u}_2^8))) \\
& +(\sin\theta_1\sin\theta_2\sin\phi)\Bigg(\frac{9}{2\sqrt{2}}\mathrm{Im}(F_1 F_2^*)(\cos\theta_2-\cos\theta_1) \\
& -\frac{9\mathsf{u}_2^2}{4}(\cos\theta_1+\cos\theta_2)\Bigg(\mathrm{Im}(F_3 F_4^*)\frac{1}{\mathsf{w}}-\sqrt{3}\mathrm{Im}(F_L F_M^*)\frac{1}{\mathsf{v}}\Bigg)\Bigg) \\
& +(\sin\theta_1\sin\theta_2\cos\phi)\Bigg(\mathrm{Re}(F_1 F_M^*)(\cos\theta_1-\cos\theta_2)\Bigg(-\frac{9M_H\mathsf{u}_1}{\sqrt{2}\mathsf{v}}\Bigg) \\
& -\frac{9\mathsf{u}_2^2}{4}(\cos\theta_1+\cos\theta_2)\Bigg(\sqrt{3}\mathrm{Re}(F_3 F_M^*)\frac{1}{\mathsf{v}}-\mathrm{Re}(F_4 F_L^*)\frac{1}{\mathsf{w}}\Bigg)\Bigg) \\
& +\eta^2\Bigg(\frac{9}{4\mathsf{u}_1^2\mathsf{v}^2\mathsf{w}^2}(\sin\theta_1\sin\theta_2\cos\phi)(\sqrt{2}\mathsf{u}_1^2\mathsf{v}^2\mathsf{w}^2\mathrm{Re}(F_1 F_2^*)-\mathsf{u}_2^4\mathsf{v}^2\mathsf{w}\mathrm{Re}(F_3 F_4^*)+\sqrt{3}\mathsf{u}_2^4\mathsf{v}\mathsf{w}^2\mathrm{Re}(F_L F_M^*) \\
& +\sqrt{q_1^2 q_2^2}(\mathsf{v}^2\mathsf{w}^2(|F_3|^2-|F_L|^2)-\mathsf{u}_2^4(|F_4|^2\mathsf{v}^2-3|F_M|^2\mathsf{w}^2))) \\
& +\frac{9}{4\mathsf{u}_1^2\mathsf{v}\mathsf{w}}(\sin\theta_1\sin\theta_2\sin\phi)(2\sqrt{2}M_H\mathsf{u}_1^3\mathsf{w}\mathrm{Im}(F_1 F_M^*)+2\sqrt{q_1^2 q_2^2}\mathsf{v}\mathsf{w}\mathrm{Im}(F_3 F_L^*) \\
& +\mathsf{u}_2^4(-\sqrt{3}\mathsf{w}\mathrm{Im}(F_3 F_M^*)-\mathsf{v}\mathrm{Im}(F_4 F_L^*)-2\sqrt{3}\sqrt{q_1^2 q_2^2}\mathrm{Im}(F_4 F_M^*)))+\frac{9}{4}\cos\theta_1\cos\theta_2\Bigg(-|F_2|^2+|F_4|^2\frac{2M_H^2\mathsf{u}_1^2}{\mathsf{w}^2} \\
& -|F_M|^2\frac{\mathsf{u}_1^2}{\mathsf{v}^2\mathsf{w}^2 X^2}(2M_H^6\mathsf{u}_1^2-M_H^4(3q_1^2+q_2^2)(q_1^2+3q_2^2)+\mathsf{u}_2^8)\Bigg)\Bigg). \qquad \text{(A1)}
\end{aligned}
$$

[1] G. Aad *et al.* (ATLAS Collaboration), Phys. Lett. B **716**, 1 (2012).
[2] G. Aad *et al.* (ATLAS Collaboration), Science **338**, 1576 (2012).
[3] S. Chatrchyan *et al.* (CMS Collaboration), Phys. Lett. B **716**, 30 (2012).
[4] S. Chatrchyan *et al.* (CMS Collaboration), Science **338**, 1569 (2012).
[5] S. Chatrchyan *et al.* (CMS Collaboration), Phys. Rev. Lett. **110**, 081803 (2013).
[6] C. A. Nelson, Phys. Rev. D **30**, 1937 (1984).
[7] J. R. Dell'Aquila and C. A. Nelson, Phys. Rev. D **33**, 80 (1986).
[8] C. A. Nelson, Phys. Rev. D **37**, 1220 (1988).
[9] M. Kramer, J. H. Kuhn, M. L. Stong, and P. M. Zerwas, Z. Phys. C **64**, 21 (1994).
[10] V. D. Barger, K.-M. Cheung, A. Djouadi, B. A. Kniehl, and P. M. Zerwas, Phys. Rev. D **49**, 79 (1994).
[11] J. F. Gunion and X.-G. He, Phys. Rev. Lett. **76**, 4468 (1996).
[12] D. J. Miller, S. Y. Choi, B. Eberle, M. M. Muhlleitner, and P. M. Zerwas, Phys. Lett. B **505**, 149 (2001).
[13] G. R. Bower, T. Pierzchala, Z. Was, and M. Worek, Phys. Lett. B **543**, 227 (2002).
[14] S. Y. Choi, in *10th International Conference on Supersymmetry*, Hamburg, DESY, 2002, edited by P. Nath, P. M. Zerwas, and C. Grosche (unpublished).
[15] S. Y. Choi, D. J. Miller, M. M. Muhlleitner, and P. M. Zerwas, Phys. Lett. B **553**, 61 (2003).
[16] R. M. Godbole, S. D. Rindani, and R. K. Singh, Phys. Rev. D **67**, 095009 (2003); Phys. Rev. D **71**, 039902(E) (2005).

[17] C. P. Buszello, I. Fleck, P. Marquard, and J. J. van der Bij, Eur. Phys. J. C **32**, 209 (2004).
[18] K. Desch, Z. Was, and M. Worek, Eur. Phys. J. C **29**, 491 (2003).
[19] M. Worek, Acta Phys. Pol. B **34**, 4549 (2003).
[20] A. B. Kaidalov, V. A. Khoze, A. D. Martin, and M. G. Ryskin, Eur. Phys. J. C **31**, 387 (2003).
[21] R. M. Godbole, S. Kraml, M. Krawczyk, D. J. Miller, P. Niezurawski, and A. F. Zarnecki, arXiv:hep-ph/0404024.
[22] C. P. Buszello and P. Marquard, arXiv:hep-ph/0603209.
[23] H. Przysiezniak, arXiv:hep-ex/0605069.
[24] M. Bluj, Report No. CMS-NOTE-2006-094.
[25] P. S. Bhupal Dev, A. Djouadi, R. M. Godbole, M. M. Muhlleitner, and S. D. Rindani, Phys. Rev. Lett. **100**, 051801 (2008).
[26] R. M. Godbole, D. J. Miller, and M. M. Muhlleitner, J. High Energy Phys. 12 (2007) 031.
[27] R. M. Godbole, P. S. Bhupal Dev, A. Djouadi, M. M. Muhlleitner, and S. D. Rindani, in *2007 International Linear Collider Workshop*, edited by A. Frey and S. Riemann, eConf C 0705302, TOP08 (2007).
[28] Y. Gao, A. V. Gritsan, Z. Guo, K. Melnikov, M. Schulze, and N. V. Tran, Phys. Rev. D **81**, 075022 (2010).
[29] C. Englert, C. Hackstein, and M. Spannowsky, Phys. Rev. D **82**, 114024 (2010).
[30] O. J. P. Eboli, C. S. Fong, J. Gonzalez-Fraile, and M. C. Gonzalez-Garcia, Phys. Rev. D **83**, 095014 (2011).
[31] U. De Sanctis, M. Fabbrichesi, and A. Tonero, Phys. Rev. D **84**, 015013 (2011).
[32] S. Berge, W. Bernreuther, B. Niepelt, and H. Spiesberger, Phys. Rev. D **84**, 116003 (2011).
[33] M. C. Kumar, P. Mathews, A. A. Pankov, N. Paver, V. Ravindran, and A. V. Tsytrinov, Phys. Rev. D **84**, 115008 (2011).
[34] J. Ellis and D. S. Hwang, J. High Energy Phys. 09 (2012) 071.
[35] C. Englert, M. Spannowsky, and M. Takeuchi, J. High Energy Phys. 06 (2012) 108.
[36] A. Bredenstein, A. Denner, S. Dittmaier, and M. M. Weber, Phys. Rev. D **74**, 013004 (2006).
[37] J. Ellis, D. S. Hwang, V. Sanz, and T. You, J. High Energy Phys. 11 (2012) 134.
[38] J. Ellis, R. Fok, D. S. Hwang, V. Sanz, and T. You, Eur. Phys. J. C **73**, 2488 (2013).
[39] P. P. Giardino, K. Kannike, M. Raidal, and A. Strumia, Phys. Lett. B **718**, 469 (2012).
[40] S. Y. Choi, M. M. Muhlleitner, and P. M. Zerwas, Phys. Lett. B **718**, 1031 (2013).
[41] R. Boughezal, T. J. LeCompte, and F. Petriello, arXiv:1208.4311.
[42] S. Banerjee, J. Kalinowski, W. Kotlarski, T. Przedzinski and Z. Was, Eur. Phys. J. C **73**, 2313 (2013).
[43] P. Avery, D. Bourilkov, M. Chen, T. Cheng, A. Drozdetskiy, J. S. Gainer, A. Korytov, K. T. Matchev *et al.*, Phys. Rev. D **87**, 055006 (2013).
[44] B. Coleppa, K. Kumar, and H. E. Logan, Phys. Rev. D **86**, 075022 (2012).
[45] C.-Q. Geng, D. Huang, Y. Tang, and Y.-L. Wu, Phys. Lett. B **719**, 164 (2013).
[46] J. Ellis, V. Sanz, and T. You, Phys. Lett. B **726**, 244 (2013).
[47] J. Frank, M. Rauch, and D. Zeppenfeld, Phys. Rev. D **87**, 055020 (2013).
[48] A. Djouadi, R. M. Godbole, B. Mellado, and K. Mohan, Phys. Lett. B **723**, 307 (2013).
[49] C. Englert, D. Goncalves-Netto, K. Mawatari, and T. Plehn, J. High Energy Phys. 01 (2013) 148.
[50] D. Stolarski and R. Vega-Morales, Phys. Rev. D **86**, 117504 (2012).
[51] L. D. Landau, Dokl. Akad. Nauk Ser. Fiz. **60**, 207 (1948).
[52] C.-N. Yang, Phys. Rev. **77**, 242 (1950).
[53] G. Kramer and T. F. Walsh, Z. Phys. **263**, 361 (1973).
[54] K. Cheung and T.-C. Yuan, Phys. Rev. Lett. **108**, 141602 (2012).
[55] Z. Chacko, R. Franceschini, and R. K. Mishra, J. High Energy Phys. 04 (2013) 015.
[56] H. de Sandes and R. Rosenfeld, Phys. Rev. D **85**, 053003 (2012).
[57] H. Kubota and M. Nojiri, Phys. Rev. D **87**, 076011 (2013).
[58] B. Grzadkowski, J. F. Gunion, and M. Toharia, Phys. Lett. B **712**, 70 (2012).
[59] V. Barger, M. Ishida, and W.-Y. Keung, Phys. Rev. Lett. **108**, 101802 (2012).
[60] T. G. Rizzo, J. High Energy Phys. 06 (2002) 056.
[61] T. Han, J. D. Lykken, and R.-J. Zhang, Phys. Rev. D **59**, 105006 (1999).
[62] R. Fok, C. Guimaraes, R. Lewis, and V. Sanz, J. High Energy Phys. 12 (2012) 062.
[63] A. Alves, Phys. Rev. D **86**, 113010 (2012).
[64] G. Aad *et al.* (ATLAS Collaboration), Phys. Lett. B **726**, 120 (2013).
[65] S. Chatrchyan *et al.* (CMS Collaboration), Phys. Rev. Lett. **110**, 081803 (2013).
[66] S. Bolognesi, Y. Gao, A. V. Gritsan, K. Melnikov, M. Schulze, N. V. Tran, and A. Whitbeck, Phys. Rev. D **86**, 095031 (2012).
[67] M. Jacob and G. C. Wick, Ann. Phys. (N.Y.) **281**, 774 (2000).
[68] S.-U. Chung, Brookhaven Nat. Lab., Report No. CERN-71-08, 2008, updated version.
[69] J. Alwall, M. Herquet, F. Maltoni, O. Mattelaer, and T. Stelzer, J. High Energy Phys. 06 (2011) 128.
[70] T. Sjostrand, L. Lonnblad, S. Mrenna, and P. Z. Skands, arXiv:hep-ph/0308153.
[71] PGS 4, http://www.physics.ucdavis.edu/~conway/research/software/pgs/pgs4-general.htm.
[72] A. Alloul, N. D. Christensen, C. Degrande, C. Duhr, and B. Fuks, arXiv:1310.1921.
[73] J. Pumplin, D. R. Stump, J. Huston, H. L. Lai, P. M. Nadolsky, and W. K. Tung, J. High Energy Phys. 07 (2002) 012.
[74] ATLAS Collaboration, Report No. ATLAS-CONF-2013-013, http://cds.cern.ch/record/1523699.
[75] LHC Higgs Cross Section Working Group, https://twiki.cern.ch/twiki/bin/view/LHCPhysics/CrossSectionsCalc.
[76] J. M. Campbell, R. K. Ellis, and C. Williams, MCFM, http://mcfm.fnal.gov.